Table S1. Keio mutants defective in stimulating larval growth and molting.

defective subclass	JW#	gene name	gene description	functional category	recovered from water?[a]	recovered from larvae?[b]	conditional on inoculum density?[c]
growth	JW0794	glnQ	L-glutamine ABC transporter, ATP binding subunit	amino acid biosynthesis/transport	N	N	Y
growth	JW3706	pstS	phosphate ABC transporter, periplasmic binding protein	cofactor synthesis/transport	N	N	Y
growth	JW3730	rbsB	ribose ABC transporter, putative periplasmic binding protein	cofactor synthesis/transport	N	N	Y
growth	JW0450	ybaJ	protein that modulates Hha toxicity	stress response	N	N	Y
growth	JW1152	ymgA	protein involved in biofilm formation	stress response	N	N	NT
growth	JW0656	ybeY	endoribonuclease	stress response	N	N	Y
growth	JW0695	ybfL	predicted transposase; receptor protein	stress response	N	N	Y
growth	JW4366	yjtD	predicted rRNA methyltransferase	stress response	N	N	Y
growth	JW3822	fadB	fatty acid oxidation complex, α component	fatty acid metabolism	N	N	Y
growth	JW2880	serA	2-oxoglutarate reductase	amino acid biosynthesis/transport	N	N	Y
growth	JW0890	serC	3-phosphoserine aminotransferase	amino acid biosynthesis/transport	N	N	NT
growth	JW0854	ltaE	L-threonine aldolase	amino acid biosynthesis/transport	N	N	Y
growth	JW3975	aceA	isocitrate lyase	central metabolism	N	N	NT
growth	JW1839	eda	multifunctional aldolase/decarboxylase	central metabolism	N	N	Y
growth	JW1838	purT	phosphoribosylglycinamide formyltransferase 2	central metabolism	N	N	Y
growth	JW2471	hyfF	hydrogenase 4, component F	central metabolism	N	N	NT
growth	JW2128	dusC	tRNA-dihydrouridine synthase C	central metabolism	N	N	Y
growth	JW2466	hyfA	hydrogenase 4, component A	central metabolism	N	N	NT
growth	JW1375	ldhA	D-lactate dehydrogenase	central metabolism	N	N	Y
growth	JW1821	yebR	methionine-(*R*)-sulfoxide reductase	stress response	N	N	Y
growth	JW2133	yeiT	NADH-dependent dihydropyrimidine dehydrogenase subunit	central metabolism	N	N	Y
growth	JW2670	ygaD	ribonucleoside-diphosphate reductase 2, β subunit dimer	central metabolism	N	N	Y
growth	JW2970	yghZ	L-glyceraldehyde 3-phosphate reductase	stress response	N	N	Y
growth	JW3349	rpe	ribulose-5-phosphate 3-epimerase	central metabolism	N	N	Y
growth	JW1841	zwf	glucose-6-phosphate dehydrogenase	central metabolism	N	N	Y
growth	JW1483	ddpX	D-Ala-D-Ala dipeptidase	peptidoglycan biosynthesis/recycling	N	N	Y
growth	JW3175	mtgA	biosynthetic peptidoglycan transglycosylase	peptidoglycan biosynthesis/recycling	N	N	Y
growth	JW0427	clpP	ClpP serine protease	stress response	N	N	Y
growth	JW0865	clpS	specificity factor for ClpA-ClpP chaperone-protease complex	stress response	N	N	Y
growth	JW0885	pflA	pyruvate formate-lyase activating enzyme	central metabolism	N	N	Y
growth	JW3580	lldD	L-lactate dehydrogenase	central metabolism	N	N	Y
growth	JW1666	pykF	pyruvate kinase I	central metabolism	N	N	Y
growth	JW0807	ybiW	predicted pyruvate formate lyase	central metabolism	N	N	Y
growth	JW2213	atoS	AtoS sensory histidine kinase	regulatory process	N	N	Y
growth	JW3905	cytR	CytR DNA-binding transcriptional repressor	regulatory process	N	N	NT
growth	JW4085	dcuR	DcuR transcriptional activator	regulatory process	N	N	Y
growth	JW3195	nanR	NanR DNA-binding transcriptional dual regulator	regulatory process	N	N	Y
growth	JW0019	nhaR	NhaR transcriptional activator	regulatory process	N	N	Y
growth	JW4200	treR	TreR DNA-binding transcriptional repressor	regulatory process	N	N	Y
growth	JW0198	yafC	putative LysR family transcriptional regulator	regulatory process	N	N	Y
growth	JW0276	yagP	predicted transcriptional regulator LYSR-type	regulatory process	N	N	Y
growth	JW0310	yahD	predicted transcriptional regulator with ankyrin domain	regulatory process	N	N	Y
growth	JW3087	tdcC	serine / threonine:H^+ symporter TdcC	amino acid biosynthesis/transport	N	N	Y
growth	JW3124	yhbQ	DNA nuclease / DNA damage response protein	stress response	N	N	NT
growth	JW4233	yjgW	KpLE2 phage-like element; predicted protein	stress response	N	N	NT
growth	JW0455	ybaM	small protein involved in the cell envelope stress response	stress response	N	N	Y
growth	JW5058	yajQ	nucleotide binding protein	stress response	N	N	Y
growth	JW1252	trpA	tryptophan synthase, α subunit	amino acid biosynthesis/transport	N	N	Y
colonization	JW5092	gltI	glutamate / aspartate ABC transporter, periplasmic binding protein	amino acid biosynthesis/transport	Y	N	Y
colonization	JW0649	gltJ	glutamate / aspartate ABC transporter, membrane subunit	amino acid biosynthesis/transport	Y	N	Y
colonization	JW3419	livF	branched chain amino acid / phenylalanine ABC transporter, ATP binding	amino acid biosynthesis/transport	Y	N	Y
colonization	JW0748	modC	molybdate ABC transporter, ATP binding subunit	cofactor synthesis/transport	Y	N	Y
colonization	JW3444	nikD	nickel ABC transporter, ATP binding subunit	cofactor synthesis/transport	Y	N	Y
colonization	JW4067	phnC	phosphonate ABC transporter, ATP binding subunit	cofactor synthesis/transport	Y	N	Y
colonization	JW4066	phnD	phosphonate ABC transporter, periplasmic binding protein	cofactor synthesis/transport	Y	N	Y
colonization	JW1112	potA	putrescine / spermidine ABC transporter, ATP binding subunit	cofactor synthesis/transport	Y	N	Y
colonization	JW2653	proW	glycine betaine ABC transporter, membrane subunit	amino acid biosynthesis/transport	Y	N	Y
colonization	JW3728	rbsA	ribose ABC transporter, putative ATP binding subunit	cofactor synthesis/transport	Y	N	Y
colonization	JW0435	ybaE	putative transport protein, periplasmic-binding component of ABC superfamily	amino acid biosynthesis/transport	Y	N	Y
colonization	JW2118	yehY	glycine betaine ABC transporter, putative membrane subunit	amino acid biosynthesis/transport	Y	N	Y
colonization	JW3712	atpA	ATP synthase F_1 complex, alpha subunit	other	Y	N	Y
colonization	JW3711	atpG	ATP synthase F_1 complex, gamma subunit	other	Y	N	Y
colonization	JW0757	bioA	adenosylmethionine-8-amino-7-oxononanoate aminotransferase	cofactor synthesis/transport	Y	N	Y
colonization	JW0758	bioB	biotin synthase	cofactor synthesis/transport	Y	N	Y
colonization	JW5130	yccU	predicted CoA-binding protein with NAD(P)-binding Rossmann-fold domain	central metabolism	Y	N	Y

[a]Y: viable colonies recovered after plating 100 µl of water from larval cultures 48 h post-inoculation; N: no viable colonies recovered

[b]Y: viable colonies recovered after plating homogenates of larvae 48 h post-inoculation; N: no viable colonies recovered

[c]Y: supplementation of larval cultures with 10^5 CFU resulted in >80% of larvae molting to the second instar within 48 h; NT: not tested

defective subclass	JW#	gene name	gene description	functional category	recovered from water?[a]	recovered from larvae?[b]	conditional on inoculum density?[c]
colonization	JW2884	yliK	methylmalonyl-CoA mutase	central metabolism	Y	N	Y
colonization	JW2216	atoA	Acetyl-CoA:acetoacetyl-CoA transferase, beta subunit	fatty acid metabolism	Y	N	Y
colonization	JW2215	atoD	Acetyl-CoA:acetoacetyl-CoA transferase, alpha subunit	fatty acid metabolism	Y	N	Y
colonization	JW2218	atoB	acetyl-CoA acetyltransferase	fatty acid metabolism	Y	N	Y
colonization	JW2217	atoE	predicted short chain fatty acid transporter	fatty acid metabolism	Y	N	Y
colonization	JW5020	fadE	acyl-CoA dehydrogenase	fatty acid metabolism	Y	N	Y
colonization	JW5156	plsX	fatty acid/phospholipid synthesis protein	fatty acid metabolism	Y	N	Y
colonization	JW3841	glnA	glutamine synthetase	amino acid biosynthesis/transport	Y	N	Y
colonization	JW2872	gcvH	glycine cleavage system H protein	amino acid biosynthesis/transport	Y	N	Y
colonization	JW2871	gcvP	glycine decarboxylase	amino acid biosynthesis/transport	Y	N	Y
colonization	JW2873	gcvT	aminomethyltransferase	amino acid biosynthesis/transport	Y	N	Y
colonization	JW2535	glyA	serine hydroxymethyltransferase	amino acid biosynthesis/transport	Y	N	Y
colonization	JW1803	sdaA	L-serine deaminase I	amino acid biosynthesis/transport	Y	N	Y
colonization	JW0002	thrB	homoserine kinase	amino acid biosynthesis/transport	Y	N	Y
colonization	JW4358	ytjC	predicted phosphatase	central metabolism	Y	N	Y
colonization	JW3863	fdoI	formate dehydrogenase-O, γ subunit	central metabolism	Y	N	Y
colonization	JW2946	glcD	glycolate oxidase, predicted FAD-linked subunit	central metabolism	Y	N	Y
colonization	JW5486	glcF	glycolate oxidase, predicted iron-sulfur subunit	central metabolism	Y	N	Y
colonization	JW1220	purU	formyltetrahydrofolate deformylase	central metabolism	Y	N	Y
colonization	JW1495	ydeP	acid resistance protein	stress response	Y	N	Y
colonization	JW2303	hisP	lysine/arginine/ornithine/histidine ABC transporter, ATP binding	amino acid biosynthesis/transport	Y	N	Y
colonization	JW3606	rfaG	lipopolysaccharide glucosyltransferase I	LPS biosynthesis/modification	Y	N	Y
colonization	JW0212	lpcA	D-sedoheptulose 7-phosphate isomerase	LPS biosynthesis/modification	Y	N	Y
colonization	JW3985	pgi	phosphoglucose isomerase	LPS biosynthesis/modification	Y	N	Y
colonization	JW3595	rfaF	ADP-heptose:LPS heptosyltransferase II	LPS biosynthesis/modification	Y	N	Y
colonization	JW3601	rfaJ	UDP-glucose:(glucosyl)LPS α-1,2-glucosyltransferase	LPS biosynthesis/modification	Y	N	Y
colonization	JW3597	rfaL	O-antigen ligase	LPS biosynthesis/modification	Y	N	Y
colonization	JW3979	metH	cobalamin-dependent methionine synthase	amino acid biosynthesis/transport	Y	N	Y
colonization	JW3459	yhiN	predicted oxidoreductase with FAD/NAD(P)-binding domain	central metabolism	Y	N	Y
colonization	JW3853	yihU	3-sulfolactaldehyde reductase	stress response	Y	N	Y
colonization	JW4346	deoB	phosphopentomutase	central metabolism	Y	N	Y
colonization	JW4344	deoC	deoxyribose-phosphate aldolase	central metabolism	Y	N	Y
colonization	JW0007	talB	transaldolase B	central metabolism	Y	N	Y
colonization	JW0106	ampD	*N*-acetyl-anhydromuramyl-L-alanine amidase	peptidoglycan biosynthesis/recycling	Y	N	Y
colonization	JW0823	dacC	D-alanyl-D-alanine carboxypeptidase	peptidoglycan biosynthesis/recycling	Y	N	Y
colonization	JW5329	dacD	DD-carboxypeptidase, penicillin-binding protein 6b	peptidoglycan biosynthesis/recycling	Y	N	Y
colonization	JW5646	envC	EnvC divisome associated factor, activator of peptidoglycan hydrolases	peptidoglycan biosynthesis/recycling	Y	N	Y
colonization	JW0210	ivy	periplasmic chaperone, inhibitor of vertebrate C-type lysozyme	peptidoglycan biosynthesis/recycling	Y	N	Y
colonization	JW1181	ldcA	L,D-carboxypeptidase A	peptidoglycan biosynthesis/recycling	Y	N	Y
colonization	JW2325	mepA	murein DD-endopeptidase	peptidoglycan biosynthesis/recycling	Y	N	Y
colonization	JW1093	nagZ	β-N-acetylhexosaminidase	peptidoglycan biosynthesis/recycling	Y	N	Y
colonization	JW0851	ybjR	anhydro-N-acetylmuramoyl-L-alanine amidase	peptidoglycan biosynthesis/recycling	Y	N	Y
colonization	JW0908	ycbB	L,D-transpeptidase	peptidoglycan biosynthesis/recycling	Y	N	Y
colonization	JW5304	yebA	murein DD-endopeptidase	peptidoglycan biosynthesis/recycling	Y	N	Y
colonization	JW0111	aceF	pyruvate dehydrogenase, E2 subunit	central metabolism	Y	N	Y
colonization	JW0110	aceE	pyruvate dehydrogenase	central metabolism	Y	N	Y
colonization	JW4030	acs	acetyl-CoA synthetase (AMP-forming)	central metabolism	Y	N	Y
colonization	JW1412	aldA	aldehyde dehydrogenase A, NAD-linked	central metabolism	Y	N	Y
colonization	JW1643	gloA	glyoxalase I	central metabolism	Y	N	Y
colonization	JW0342	mhpF	acetaldehyde dehydrogenase (acylating)	central metabolism	Y	N	Y
colonization	JW2198	mqo	malate:quinone oxidoreductase	central metabolism	Y	N	Y
colonization	JW3366	pck	phosphoenolpyruvate carboxykinase (ATP)	central metabolism	Y	N	Y
colonization	JW0886	pflB	pyruvate formate-lyase (inactive)	central metabolism	Y	N	Y
colonization	JW2294	pta	phosphate acetyltransferase / phosphate propionyltransferase	central metabolism	Y	N	Y
colonization	JW0390	phoR	PhoR sensory histidine kinase	regulatory process	Y	N	Y
colonization	JW0710	gltA	citrate synthase	central metabolism	Y	N	Y
colonization	JW0112	lpd	lipoamide dehydrogenase	central metabolism	Y	N	Y
colonization	JW1253	trpB	tryptophan synthase, β subunit dimer	amino acid biosynthesis/transport	Y	N	Y
colonization	JW2317	pdxB	erythronate-4-phosphate dehydrogenase	cofactor synthesis/transport	Y	N	Y
colonization	JW2548	pdxJ	pyridoxine 5'-phosphate synthase	cofactor synthesis/transport	Y	N	Y
colonization	JW2894	epd	erythrose 4-phosphate dehydrogenase	cofactor synthesis/transport	Y	N	Y
colonization	JW1628	pdxY	pyridoxal kinase 2	cofactor synthesis/transport	Y	N	Y
rescue	JW4364	arcA	ArcA transcriptional dual regulator	regulatory process/respiration	Y	Y	-
rescue	JW0723	cydB	cytochrome *bd*-I terminal oxidase subunit II	respiration	Y	Y	-
rescue	JW0870	cydD	ATP-binding/permease protein	respiration	Y	Y	-
rescue	JW1328	fnr	FNR DNA-binding transcriptional dual regulator	regulatory process/respiration	Y	Y	-

[a]Y: viable colonies recovered after plating 100 µl of water from larval cultures 48 h post-inoculation; N: no viable colonies recovered

[b]Y: viable colonies recovered after plating homogenates of larvae 48 h post-inoculation; N: no viable colonies recovered

[c]Y: supplementation of larval cultures with 10^5 CFU resulted in >80% of larvae molting to the second instar within 48 h; NT: not tested

Table S2. Primers designed against the *E. coli* K12 BW25113 genome (NCBI Accession No. CP009273) and used to construct the Δ*cydB*-Δ*cydD::kan* and Δ*narZ*-Δ*narG::kan* double mutants.*

Name	Sequence (5'-3')	Target gene	Reference
k2	CGGTGCCCTGAATGAACTGC	*kan*	(1)
kt	CGGCCACAGTCGATGAATCC	*kan*	(1)
cydB-U	GCAGGCGATCTCATCTTCTC	*cydA*	This study
cydB-D	AAGAAGCGTTCCCAGAATCC	*cydX*	This study
cydD-U	CACCACGGAAGTGGAAAACT	*trxB*	This study
cydD-D	CGCTGATGGTCTGTCGTAGA	*cydC*	This study
narG-U	GCTTTGCAATGCTGTCAAAA	*narK*	This study
narG-D	TAACGGATACGACCGACACA	*narH*	This study
narZ-U	TTACAACGCCTGCATCTCTG	*narU*	This study
narZ-D	TTTTCTGACTTGCCGCTTTT	*narY*	This study

* Δ*cydB::kan* and Δ*narZ::kan* were transformed with pCP20, which shows thermal induction of flippase (FLP) synthesis, to excise the kanamycin resistance cassette (Kan^R) via the flanking flippase recognition target (FRT) sites while maintaining the gene deletion (56). Individual colonies were streaked on kanamycin (25 μg/ml), ampicillin (200 μg/ml), and chloramphenicol (20 μg/ml) LB agar plates and selected, followed by PCR using the k2 and kt primers to confirm loss of the Kan^R cassette and pCP20 (56). Resulting kanamycin-susceptible mutants were then transduced with P1 phage stocks generated from the desired Keio mutant (Δ*cydD::kan* and Δ*narG::kan*) to incorporate the second mutation. Four PCR reactions were then performed to verify that the Δ*cydB*-Δ*cydD::kan* and Δ*narZ*-Δ*narG::kan* mutants had the correct structure. New junctions created between the Kan^R cassette and neighboring upstream and downstream sequences were verified using the kanamycin (kt or k2) and locus-specific (U or D) primers. A third reaction was carried out using the flanking locus-specific primers (U and D) to verify simultaneous loss of the parental (non-mutant) fragment and gain of the new mutant-specific fragment. A fourth reaction using primers k2 and kt was then used to screen for the Kan^R cassette.

Table S3. Primers designed against the *E. coli* K12 BW25113 genome and used to construct the mutants Δ(*cyoA-cyoB*)*::kan,* Δ(*napA-napD*)*::kan*, and Δ*cydB-*Δ*cydD-*Δ(*cyoA-cyoB*)*::kan*.*

Name	Sequence (5'-3')	Target gene	Reference
P1	ATTCCGGGGATCCGTCGACC	*kan*-FRT	(2)
P2	TGTAGGCTGGAGCTGCTTCG	*kan*-FRT	(2)
P1-rev	GGTCGACGGATCCCCGGAAT	*kan*-FRT	(2)
P2-rev	CGAAGCAGCTCCAGCCTACA	*kan*-FRT	(2)
cyoA-U	GCTGGATTATCTGGCGCTAC	*ampG*	This study
cyoB-D	GATGGAGCTGAACAACAGCA	*cyoC*	This study
napD-U	CGCAAAGCCAGTAACGGTAT	*napF*	This study
napA-D	AGCGGTAACACCTTGATTGC	*napG*	This study

* Δ(*cyoA-cyoB*)*::kan* and Δ(*napA-napD*)*::kan* were generated by first performing three standard and one fusion PCR reaction to construct linear DNA fragments containing the Kan^R cassette and two flanking homology regions of the target genes. First, the Kan^R cassette was PCR amplified from Keio mutant genomic DNA using primers binding upstream (P1) and downstream (P2) of the flanking FRT sites. Junctions between the Kan^R cassette and neighboring upstream and downstream sequences for the target genes of interest were then PCR amplified using genomic DNA from the corresponding Keio mutants (Δ*cyoA::kan,* Δ*cyoB::kan*, Δ*napA::kan,* or Δ*napD::kan*) as template and primer pairs cyoA-U/P1-rev, cyoB-D/P2-rev, napA-D/P2-rev, or napD-U/P1-rev, respectively. Finally, PCR fragments from these reactions were assembled by fusion PCR using the flanking locus-specific primers sets cyoA-U/cyoB-D and napD-U/napA-D. Assembled PCR products were purified and electroporated into the parental BW25113 strain carrying plasmid pKD46 (56). Resulting mutants were selected on kanamycin (25 μg/ml) and ampicillin (100 μg/ml) LB agar plates to ensure loss of the pKD46 plasmid. New junctions created between the Kan^R cassette and neighboring upstream and downstream sequences were then verified for each mutation by PCR with kanamycin (kt or k2) and locus-specific (U or D) primers. The quadruple mutant Δ*cydB-*Δ*cydD-*Δ(*cyoA-cyoB*)*::kan* was generated by pCP20-mediated removal of the Kan^R cassette from the Δ*cydB-*Δ*cydD::kan* double mutant followed by transduction with the Δ(*cyoA-cyoB*)*::kan* mutation and PCR verification of the new mutant as described above.

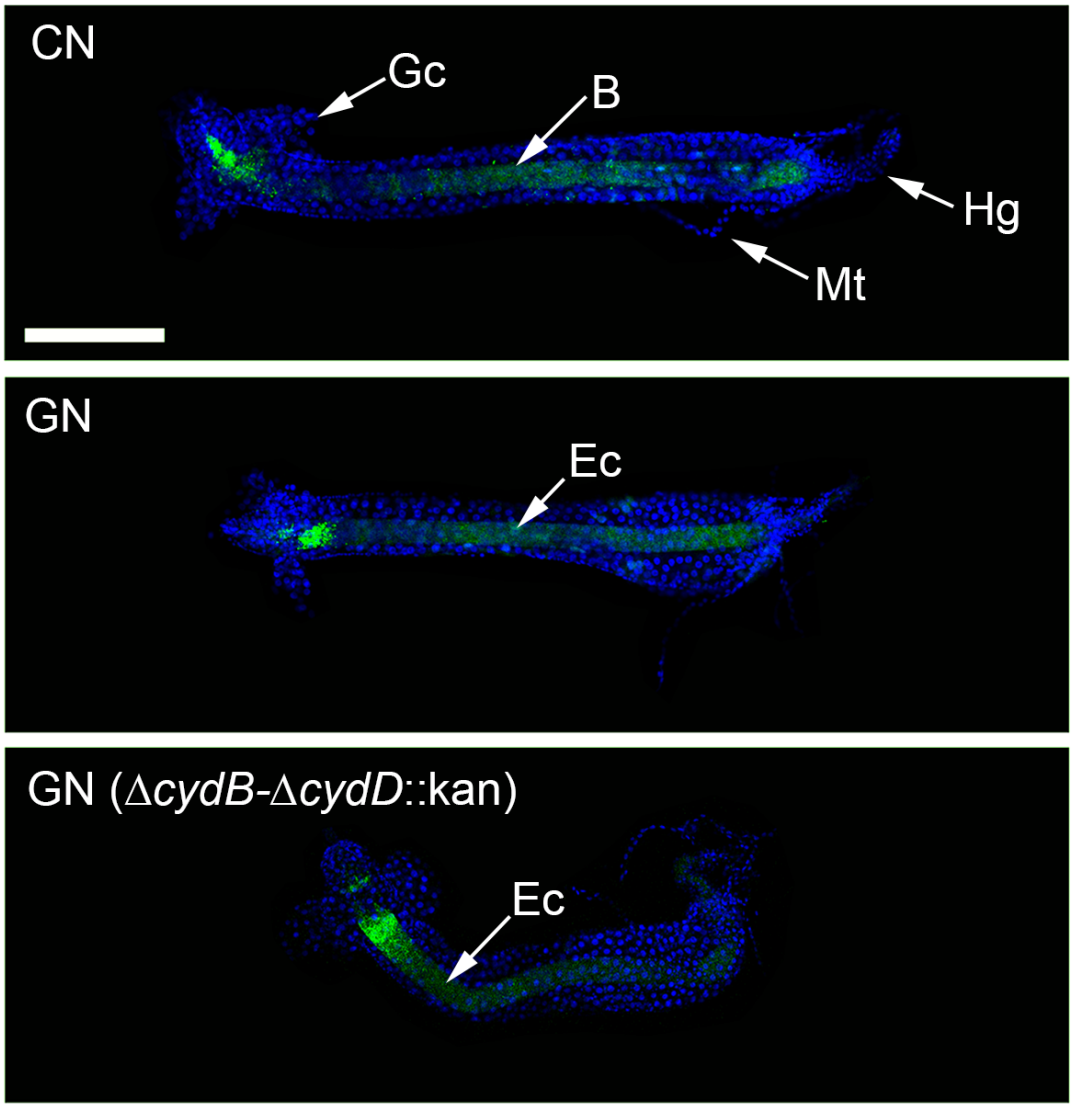

Fig. S1. Representative confocal microscopy images of midguts from conventional (CN) and gnotobiotic larvae inoculated with wild-type (GN) or Δ*cydB*-Δ*cydD*::kan *E. coli*. The foregut was removed in each image resulting in the gastric caecae (Gc), Malpighian tubules (Mt) and hindgut (Hg) being oriented left to right. Cell nuclei were stained with Hoechst 33342 (blue) while a peptidoglycan antibody (GeneTex) visualized by an Alexafluor 488 secondary antibody (green) labeled the mixed community of bacteria (B) in CN larvae and *E. coli* (Ec) in gnotobiotic larvae. Note the distribution and fluorescence intensity of bacteria is very similar across treatments. Methods for antibody labeling and confocal microscopy are as previously described (3). Scale bar in the upper panel equals 200 μm.

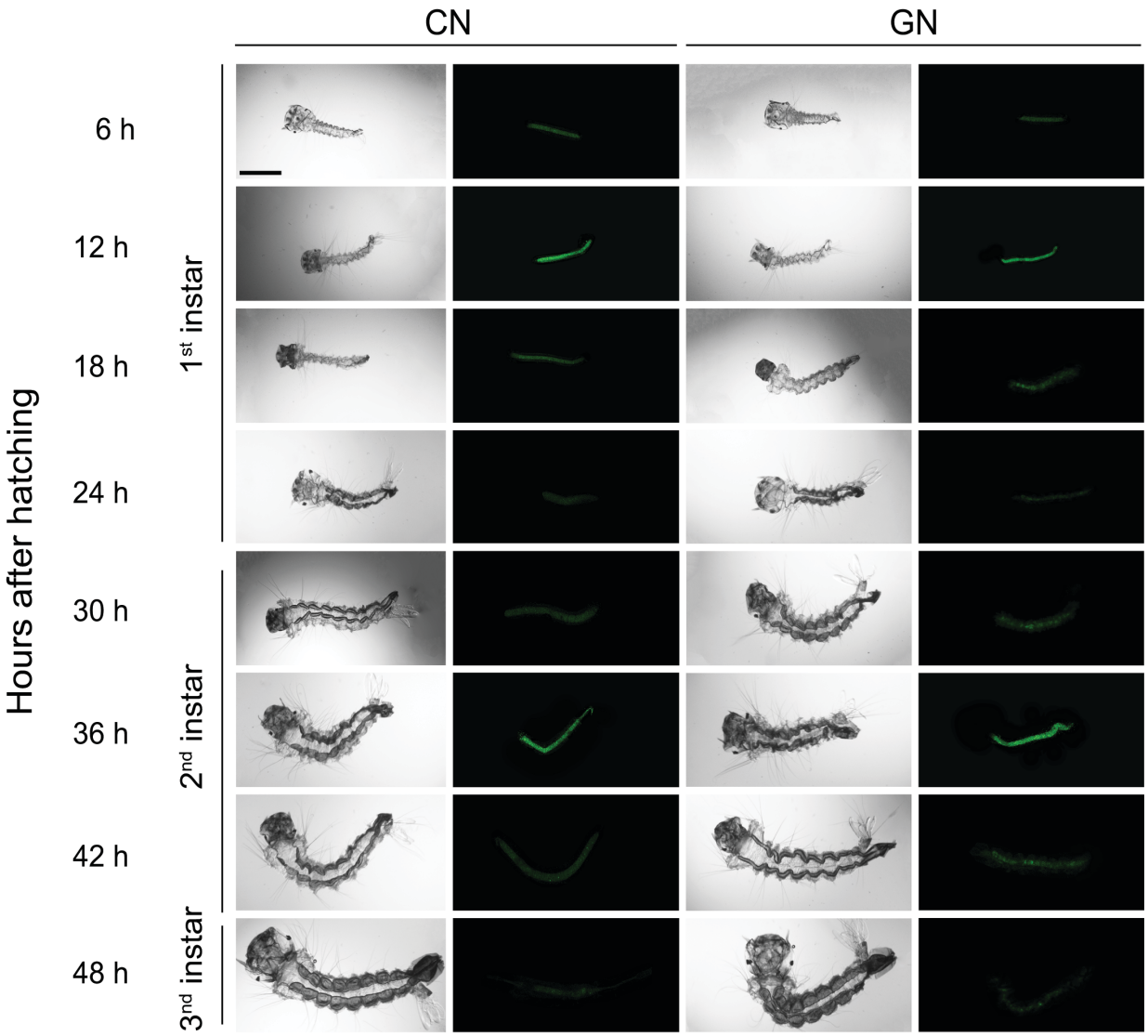

Fig. S2. Image iT fluorescence in conventional (CN) and gnotobiotic larvae inoculated by wild-type *E. coli* (GN). Individual larvae were examined by confocal microscopy from 6-48 h post-hatching. Sampling times are indicated to the left. For each treatment, the image to the left shows a light image of a larva while the right shows the corresponding fluorescence image. Anterior (head) of each larva is oriented to the left. Image iT fluorescence (green) is restricted to the midgut and is most intense in pre-critical size larvae (see main text). Scale bar in the upper left equals 500 μm. A total of 10 larvae was examined for each treatment and time point with all outcomes similar to the images shown.

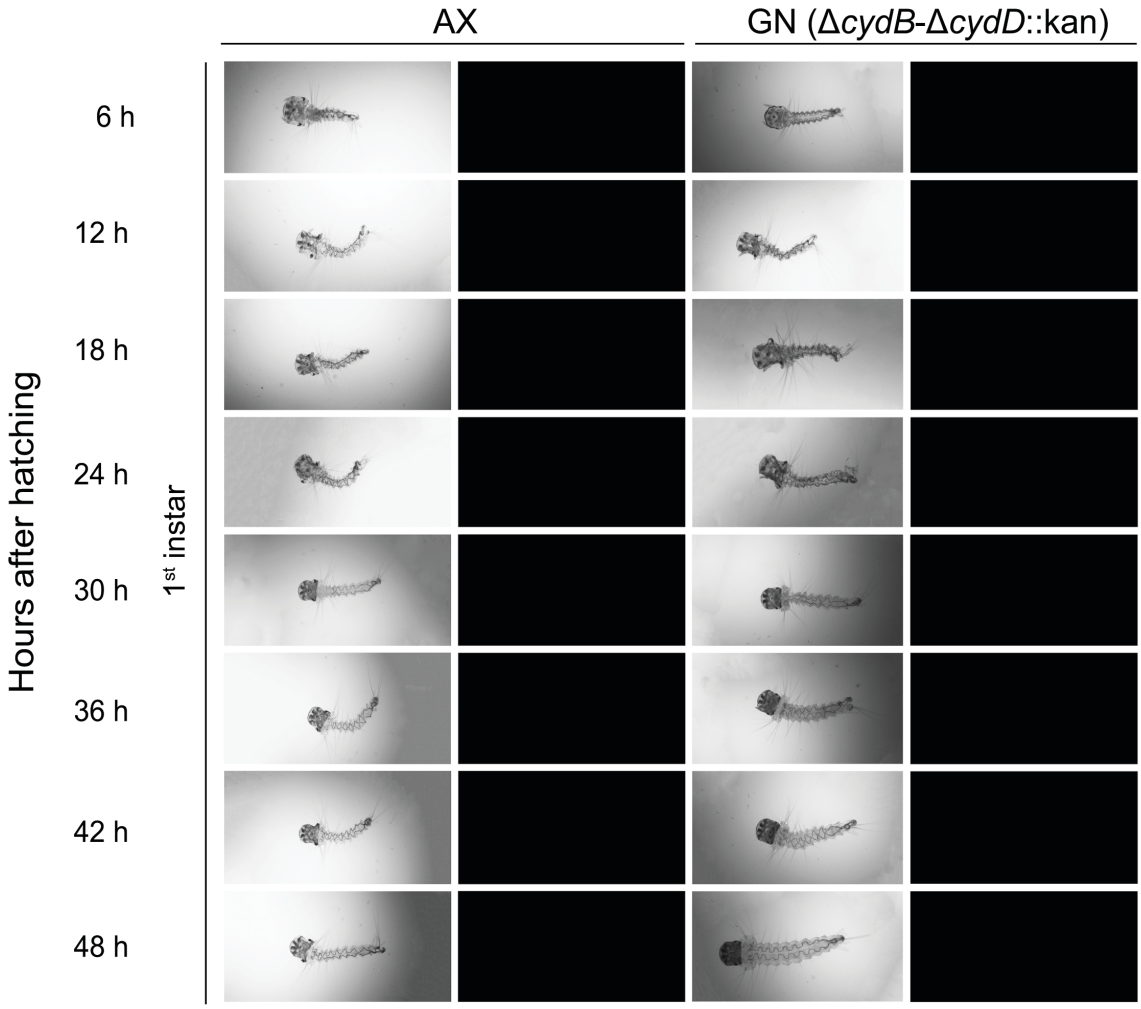

Fig. S3. Image iT fluorescence in axenic (AX) and gnotobiotic larvae inoculated with Δ*cydB*-Δ*cydD*::*kan E. coli* [GN (Δ*cydB*-Δ*cydD*::*kan*)]. Individual larvae were examined and are oriented as in Fig. S1. Note the absence of Image iT fluorescence in larvae for both treatments. A total of 10 larvae was examined for each treatment and time point with all outcomes similar to the images shown.

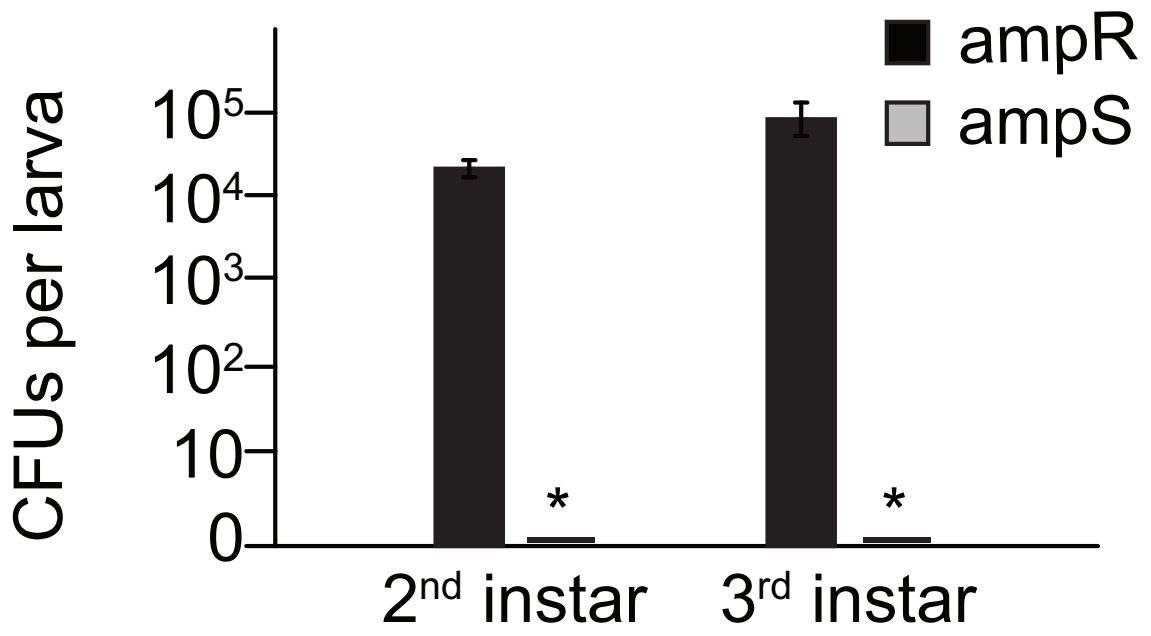

Fig. S4. Ampicillin treatment eliminated ampicillin-susceptible (ampS) *E. coli* from *Ae. aegypti* larvae while ampicillin-resistant (ampR) *E. coli* persisted. Gnotobiotic larvae inoculated with ampR and ampS *E. coli* were treated by adding ampicillin to cultures after larvae molted to the 2nd or 3rd instar. Individual larvae were subsequently homogenized 24 h post-treatment and the resulting homogenates cultured on LB plates at 37° for 24 h to determine cfu ± SE per larva. Four individual larvae were bioassayed per treatment.

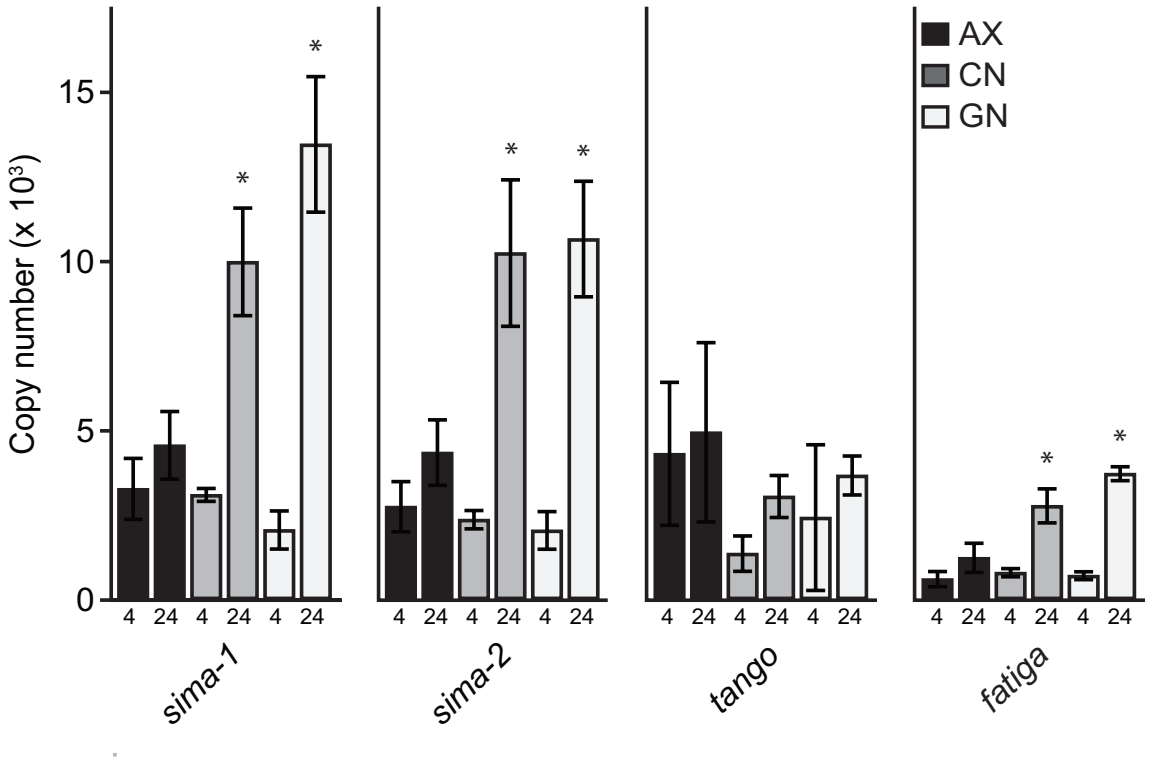

Fig. S5. Transcript copy number of *Ae. aegypti* hypoxia genes in axenic (AX), conventional (CN) and gnotobiotic first instars inoculated with wild-type *E. coli* (GN). Larvae were collected at 4 h and 24 h post-hatching followed by extraction of total RNA and RT-qPCR analysis (see Supplemental Experimental Procedures). The bars in each graph show copy number of each gene (± SE) per 500 ng of total RNA. For each gene, an asterisk (*) indicates copy number significantly differed from all other treatments and sample times ($P < 0.05$, ANOVA followed by a post-hoc Tukey-Kramer Honest Significant Difference test). A minimum of 4 independent biological replicates were analyzed per treatment and time point.

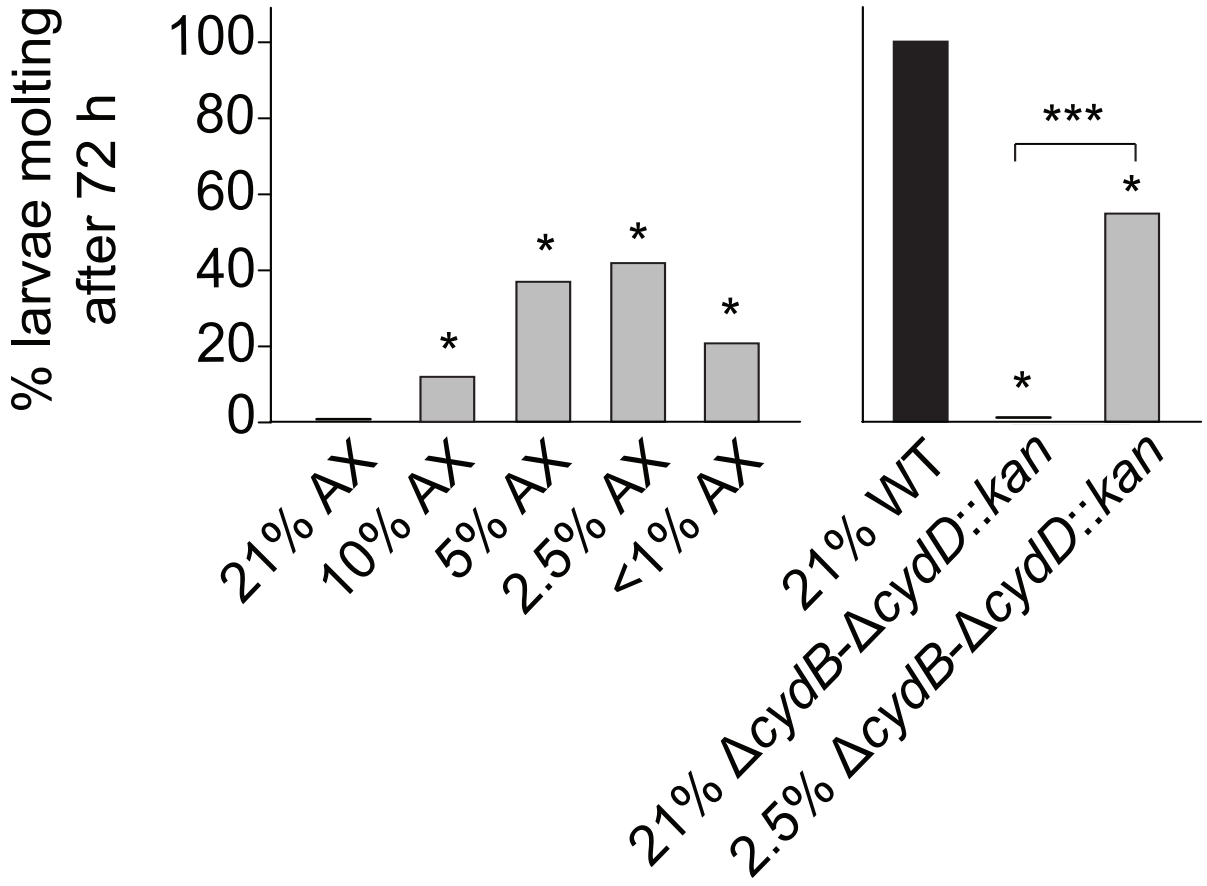

Fig. S6. Percentage of axenic (AX) or gnotobiotic larvae inoculated with Δ*cydB*-Δ*cydD*::*kan E. coli* that molted to the second instar after transient exposure to environmental hypoxia. In the left panel axenic larvae were maintained at 21% oxygen (normoxia) or exposed for 2 h to 10%-<1% oxygen. An asterisk (*) indicates a significant difference in the proportion of larvae that initiated a molt relative to larvae maintained at 21% oxygen ($P < 0.0001$, Fisher's exact test). In the right panel larvae inoculated with wild-type (WT) *E. coli* were maintained at 21% oxygen while larvae inoculated with Δ*cydB*-Δ*cydD*::*kan E. coli* were either maintained in 21% oxygen or exposed for 2 h to 2.5% oxygen. * indicates that Δ*cydB*-Δ*cydD*::*kan* larvae exposed to 21% and 2.5% oxygen differed from the WT positive control ($P < 0.0001$, Fisher's exact test). *** indicates that significantly more Δ*cydB*-Δ*cydD*::*kan* larvae exposed to 2.5% oxygen initiated a molt than Δ*cydB*-Δ*cydD*::*kan* larvae held in 21% oxygen. At least 40 larvae were assayed per treatment. Initiation of molting was based upon visually seeing the formation of new cuticle beneath the old cuticle of the larva.

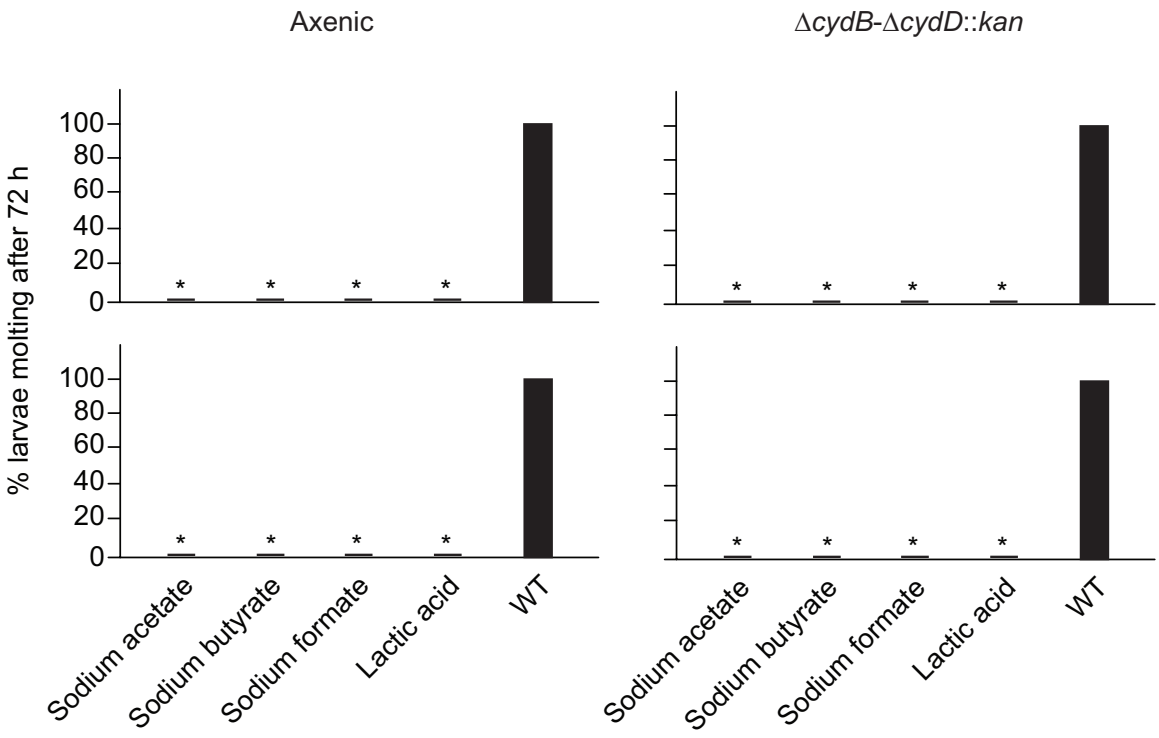

Fig. S7. Addition of sodium acetate, sodium butyrate, sodium formate or lactic acid to cultures does not induce axenic or gnotobiotic larvae inoculated with Δ*cydB*-Δ*cydD*::*kan* *E. coli* to molt. Newly hatched axenic larvae were individually placed into wells containing 1 ml of water and 100 µg of standard rearing diet plus no bacteria (Axenic) (left panel) or 1 x 10^6 Δ*cydB*-Δ*cydD*::*kan E. coli* (right panel). Sodium acetate (Sigma), sodium butyrate (Sigma), sodium formate (Sigma), or 0.2-2% (v/v) lactic acid was then added to wells at a working concentration of either 10 µM (upper panel) or 1 mM (lower panel). A minimum of 20 larvae per treatment was monitored for 72 h and the proportion of larvae that molted to the second instar was recorded. Individual larvae placed in wells containing 1 ml of water and 100 µg of standard rearing diet plus 1 x 10^6 wild-type (WT) *E. coli* served as a positive control.

Supplemental Experimental Procedures

Measurement of 20E Titers by EIA. Thirty staged first instars per sample were homogenized in 400 µl of 5% aqueous methanol and centrifuged. Each supernatant was added to a C_{18} solid phase extraction column (Phenomenex), while the pellet was washed with 500 µl of 5% aqueous methanol, re-centrifuged, and added to the same C_{18} column. After rinsing with one volume of 5% methanol, ecdysteroids were eluted with 1 ml of 100% methanol, evaporated to dryness, and stored at -80° C. Samples were rehydrated with cold phosphate-buffered saline and analyzed by enzyme immunoassay (EIA) (60) in 96-well plates (Costar). Plate wells were coated with an ecdysone-lactoglobulin conjugate. Sample medium (50 µl) or 20E standards (4-2000 pg) were added to wells followed by affinity purified ecdysone antiserum (50 µl, 1:2,500 final dilution). After washing, a horseradish peroxidase-conjugated goat anti-rabbit secondary antibody (Sigma) was added, followed by rinsing, and addition of substrate (3,30,5,5'-tetramethylbenzidine) (KPL). After stopping the reaction with an equal volume of 1 M phosphoric acid, absorbance was measured at 450 nm using a plate reader (Biotek) followed by determination of ecdysone concentration in each sample relative to the standard curve.

RT-qPCR Analysis of *Ae. aegypti* Hypoxia Genes. Total RNA was extracted from 10 larvae per treatment using the Qiagen RNEasy mini kit following the manufacturer's instructions. Following the extraction, RNA was subject to DNAse treatment using the Turbo DNA-free kit (Life Technologies). cDNA was then synthesized using 500 ng of total RNA using the BioRad iScript cDNA synthesis kit. The following primers were used for qPCR:

AAEL001097-forward (*hifα/sima1*) GAAATGTTGCCAATGGTGAA
AAEL001097-reverse (*hifα/sima1*) GGTAATATCCCCATCAGCAG
AAEL015383-forward (*hifα/sima2*) GAAATGTTGCCAATGGTGAA
AAEL015383-reverse (*hifα/sima2*) GAGAGTAGGGCTAGCTTTTC
AAEL010343-forward (*hifβ/tango*) CAGATGTTTTCGGTGATGTAC
AAEL010343-reverse (*hifβ/tango*) TACACACCACGTACTCAATG
AAEL002798-forward (*fatiga*) GGGAACAATAGTGGTTACAGT
AAEL002798-reverse (*fatiga*) GAGTTAACTGCATTTCACCTC
AAEL000741-forward (*e74*) GAAGTCCCAGATTCCTACTAC
AAEL000741-reverse (*e74*) TAGCGGATGTTCTTCTTTGAT
AAEL009496-forward (ribosomal protein S7) ACCGCCGTCTACGATGCCA
AAEL009496-reverse (ribosomal protein S7) ATGGTGGTCTGCTGGTTCTT.

PCR products were amplified from cDNA and cloned into the vector pSC-A using the Strataclone kit (Agilent). Inserts were sequenced to verify product length and to determine copy number then serially diluted to produce standard curves for each gene using qPCR. Four biological replicates for each treatment and time point were run in four technical replicates on a Rotor Gene-Q (Qiagen) using RT² SYBR Green qPCR Mastermix (Qiagen) according to the manufacturer's instructions. Ribosomal protein S7 expression levels were used to normalize values between samples.

References

1. Datsenko KA, Wanner BL (2000) One-step inactivation of chromosomal genes in Escherichia coli K-12 using PCR products. *Proc Natl Acad Sci USA 97*(12):6640-6645.
2. Baba T, Ara T, Hasegawa M, Takai Y, Okumura Y, Baba M, Datsenko KA,Tomita M, Wanner BL, Mori H (2006) Construction of Escherichia coli K-12 in-frame, single-gene knockout mutants: the Keio collection. *Mol Syst Biol* doi:10.1038/msb4100050.
3. Vogel KJ, Valzania L, Coon KL, Brown MR, Strand MR (2017) Transcriptome sequencing reveals large-scale changes in axenic Aedes aegypti larvae. *PLoS Negl Trop Dis* 11(1):e0005273.